

CU-Net: Efficient Point Cloud Color Upsampling Network

Lingdong Wang
 University of Massachusetts Amherst
 Amherst, Massachusetts, USA

Jacob Chakareski
 New Jersey Institute of Technology
 Newark, New Jersey, USA

Mohammad Hajiesmaili
 University of Massachusetts Amherst
 Amherst, Massachusetts, USA

Ramesh K. Sitaraman
 University of Massachusetts Amherst
 Amherst, Massachusetts, USA

Abstract

Point cloud upsampling is necessary for Augmented Reality, Virtual Reality, and telepresence scenarios. Although the geometry upsampling is well studied to densify point cloud coordinates, the upsampling of colors has been largely overlooked. In this paper, we propose CU-Net, the first deep-learning point cloud color upsampling model. Leveraging a feature extractor based on sparse convolution and a color prediction module based on neural implicit function, CU-Net achieves linear time and space complexity. Therefore, CU-Net is theoretically guaranteed to be more efficient than most existing methods with quadratic complexity. Experimental results demonstrate that CU-Net can colorize a photo-realistic point cloud with nearly a million points in real time, while having better visual quality than baselines. Besides, CU-Net can adapt to an arbitrary upsampling ratio and unseen objects. Our source code will be released to the public soon.

1. Introduction

Point cloud is a fundamental 3D representation. Dense point clouds are required by many applications like rendering, surface reconstruction, and semantic understanding in augmented/virtual reality (AR/VR) [3, 11, 42] as well as telepresence [8, 26, 40, 43]. Unfortunately, hardware and computational constraints in capturing, compressing, and processing point clouds always lead to sparse ones. Therefore, point cloud upsampling technique is essential to the densification of point clouds.

Existing works [1, 9, 13, 20, 21, 31–33, 38, 39, 41] have developed point cloud **geometry upsampling** to increase the number of point coordinates, but largely ignored the color attributes associated with points. We argue that an

efficient and scalable **color upsampling** is critical in many telepresence scenarios. For example, during 3D video conferencing or remote collaboration, a human avatar represented as a colored point cloud with millions of points needs to be streamed in real time. It's infeasible to transfer the full data given today's compression standards [10] and network bandwidth. One potential solution is to stream a degraded low-quality point cloud and then upsample it as post-processing. Colors of the human avatar must be carefully treated during upsampling, as artifact or blurs on human face can lead to the uncanny valley effect and severely harm the visual quality. This motivates us to develop a color upsampling method that can process millions of points in real time with satisfying perceptual performance.

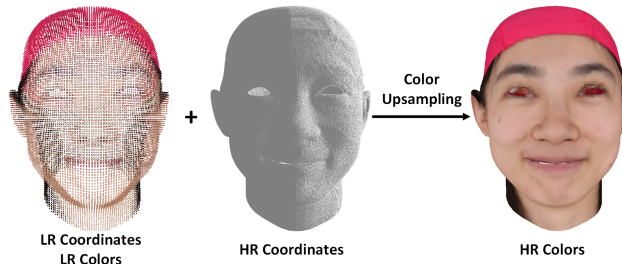


Figure 1. Point cloud color upsampling task.

In this project we focus on point cloud color upsampling, which can be applied after an existing geometry upsampling like PU-Dense [1]. Color upsampling could be viewed as the generalization of super resolution from 2D to 3D. As shown in Fig. 1, the inputs are a low-resolution (LR) sparse point cloud with both point coordinates and colors, and a high-resolution (HR) dense point cloud with merely coordinates. The output is a set of colors for the HR point cloud. This task has only been tackled by sim-

ple rule-based methods [4, 42] and inefficient optimization-based methods [7, 16] before. Here we propose CU-Net, the first deep-learning point cloud color upsampling method to the best of our knowledge.

Efficient operation is the major challenge in achieving real-time processing of large-scale point clouds. In particular, though most upsampling methods existing in practice process only point coordinates, they can only work with a small-scale point cloud having thousands of points. When applied to a large-scale cloud with millions of points, these methods have to follow a divide-and-merge pattern and consume tens of minutes [1] due to their poor memory and runtime efficiency. Besides, tiling of the large-scale point cloud introduces boundary artifact and decreases the visual quality.

The inefficiency of existing upsampling methods is rooted in their $O(N_l^2)$ or even $O(N_h^2)$ complexity, where N_l is the size of the LR point cloud and N_h is the size of the HR point cloud. Such quadratic complexity usually comes from the deep-learning feature extractors they adopt, like PointNet++ [30], Dynamic Graph CNN (DGCNN) [36], Graph Convolutional Network (GCN) [13, 31], or Transformer [12, 44]. We comprehensively analyze the complexity of existing methods in Sec. 2.1.

To pursue low complexity, four efficient modules comprise our proposed framework CU-Net: feature extraction, feature expansion, color prediction, and devoxelization. An illustration of the workflow is given in Fig. 2. The feature extraction module firstly extracts deep-learning color features for the LR point clouds, namely LR features. Then the feature expansion module expands the LR features towards HR point cloud to be HR features. Next, the color prediction module transforms HR features into residual colors. Eventually, the devoxelization module generates coarse HR colors, which are added with the previously learned residuals to be the final output.

We carefully design each module of CU-Net to achieve efficiency and scalability. Our feature extraction module is based on sparse convolution [6, 35], the color prediction module forms a neural implicit function (or neural field) [9, 25], and the other two modules are composed of basic matrix operations. After all, CU-Net achieves $O(N_h)$ time and space complexity, which is theoretically guaranteed to be more efficient than most prior works. A detailed explanation to the complexity is available in Sec. 3.5. Besides, the neural implicit function design allows CU-Net to be used for an arbitrary upsampling ratio without retraining.

We summarize our contributions as follow:

1. We propose CU-Net, the first deep-learning model for point cloud color upsampling.
2. CU-Net is efficient in terms of runtime, memory consumption, and storage space. With $O(N_h)$ time

and space complexity, CU-Net can colorize a photo-realistic point cloud with nearly a million points within 30ms latency using a 3MB model.

3. CU-Net supports arbitrary-ratio color upsampling. One model can adapt to different upsampling ratios, which avoids retraining and storing multiple models.
4. Through abundant experiments, we verify that CU-Net significantly outperforms baselines in visual quality both quantitatively and qualitatively. CU-Net also best other methods when generalized to unseen objects.

2. Related Works

2.1. Deep Learning in Point Cloud

Following the success in 2D computer vision, deep learning has shown great potential in processing 3D point clouds, especially extracting meaningful features. There are generally five kinds of deep-learning feature extractors for point clouds, namely PointNet++ [30], Dynamic Graph CNN (DGCNN) [36], Graph Convolutional Network (GCN) [13, 31], Transformer [12, 44], and sparse-convolution-based model [6, 35].

The first four methods all have $O(N^2)$ complexity. PointNet++ recursively computes ball query around all points, and then applies PointNet [29] to learn hierarchical features of point cloud. DGCNN computes K-Nearest Neighbor (KNN) multiple times to dynamically construct graphs among features and aggregate features via edge convolution. Both ball query and KNN are implemented as $O(N^2)$ on GPU for parallelism. GCN transforms the point cloud into a KNN graph and then performs graph convolution. Graph convolution is $O(N^2)$ as it consumes adjacent matrices. Transformer employs self-attention mechanism to capture relationships among all points, and the computation of attention is $O(N^2)$.

Sparse convolution is the only feature extractor with $O(N)$ complexity. Sparse convolution resembles traditional 3D convolution, but exploits the sparsity of point clouds. Specifically, it stores the quantized positions of all points via a hash map, and then performs convolution only on the position where a point exists. MinkowskiEngine [6] is a widely-used framework for sparse convolution. While TorchSparse [35] achieves 1.6 \times speedup towards MinkowskiEngine by balancing the irregular computation workload and reducing memory footprint. In this project, we adopt TorchSparse to implement our feature extractor.

2.2. Point Cloud Upsampling

Point cloud geometry upsampling is formulated as an optimization problem in pioneering works [2, 17, 18, 22], but they are recently outperformed by deep-learning methods.

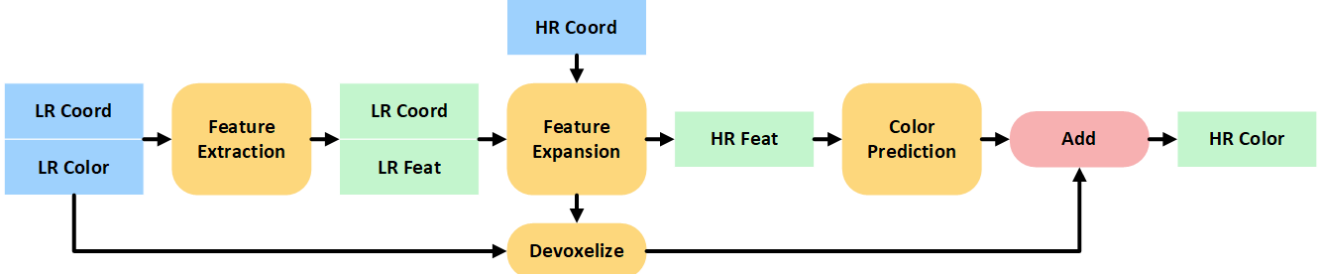


Figure 2. Workflow of CU-Net.

PU-Net [41] is the first deep-learning geometry upsampling model. It extracts features with PointNet++ [30] and expands the point cloud using multi-branch Multi-Layer Perceptron (MLP). 3PU [39] adopts DGCNN [36] as feature extractor and upsamples point cloud in a patch-based progressive way. With the same feature extractor, PU-GAN [20] proposes a Generative Adversarial Network (GAN) to upsample points. Dis-PU [21] firstly generates a dense but coarse point cloud and then refines the locations. PU-GCN [31] employs graph convolution for feature extraction and a novel NodeShuffle module for upsampling. PU-GACNet [13] further introduces attention mechanism into graph convolution to capture global-range relations. PU-Transformer [33] develops a multi-head self-attention module with shifted channels to extract features. PU-Dense [1] adopts a U-Net feature extractor based on sparse convolution. Due to the efficient sparse convolution, it can process large-scale point clouds much faster than other methods.

Some geometry upsampling methods support arbitrary-ratio upsampling. Meta-PU [38] employs meta-learning to predict the weight of graph convolution kernels in adaptation to different ratios. Yue *et al.* [32] interpolates points through an affine combination of neighboring points projected onto the tangent plane and a further refinement. NeuralPoints [9] transforms a 2D square patch to fit a 3D local surface through a neural implicit function [25], which allows the model to sample any number of points from the surface. With a similar design, CU-Net also supports arbitrary-ratio upsampling.

Only a few point cloud upsampling methods considered colors. YuZu [42] develops a volumetric video streaming system based on point cloud upsampling. It upsamples colors with Nearest Neighbor (NN), which will leave patch artifact. Tomás *et al.* [4] organize the point cloud as an octree, and then utilize a look-up table to pair neighborhood configurations with child occupancy. It colorizes a LR voxel using Weighted Average of Nearest Neighbors (WAAN), the weighted average color of parent voxels sharing an edge with it. But such interpolation generates blurry texture. FS-MMR [16] projects 3D point cloud to 2D surface by constructing a graph and computing a minimum-spanning tree.

It then interpolates colors on the 2D surface by optimizing the coefficients of frequency basis functions. FGTV [7] transforms the point cloud into a KNN graph, and minimizes a weighted L_1 norm on colors through linear programming. Optimization-based methods like FSMMR and FGTV can only run on CPU with unacceptably high latency on large-scale point clouds. In contrast, our deep-learning model CU-Net can be accelerated by GPU to generate high-fidelity colors for large-scale point clouds in real time.

2.3. Colors of Point Cloud

Other than color upsampling, several topics investigate colors in point clouds. Point cloud colorization methods [5, 23, 34] leverage GAN to generate colors for an uncolored point cloud. However, it's highly ambiguous to colorize a point cloud without any guidance. In contrast, color upsampling colorizes point clouds under the supervision of LR colors, thus returns more reasonable results. Point cloud completion aims at completing a missing part of an object. Yuki *et al.* [19] adopts GAN to complete a haired human head, but the target point cloud is in small scale with few thousands of points. Point cloud color upsampling could be viewed as the completion of scattered points instead of a whole part. Hence color upsampling cares more about low-level local information instead of high-level semantics.

3. Proposed Method

The workflow of our point cloud color upsampling model CU-Net is illustrated in Fig. 2. Our model accepts a low-resolution (LR) point cloud with both coordinates and colors and a high-resolution (HR) point cloud with only coordinates. And it generates colors for the HR point cloud.

CU-Net starts with the **feature extraction** module, which extracts deep-learning color features from the LR point clouds. The LR features are then expanded into HR features by the **feature expansion** module. The HR features will be transformed into color residuals of the HR point cloud by the **color prediction** module. Eventually, the **devoxelization** module outputs coarse HR colors, which form the final HR colors together with previously learned residu-

als. Details of these modules are introduced below.

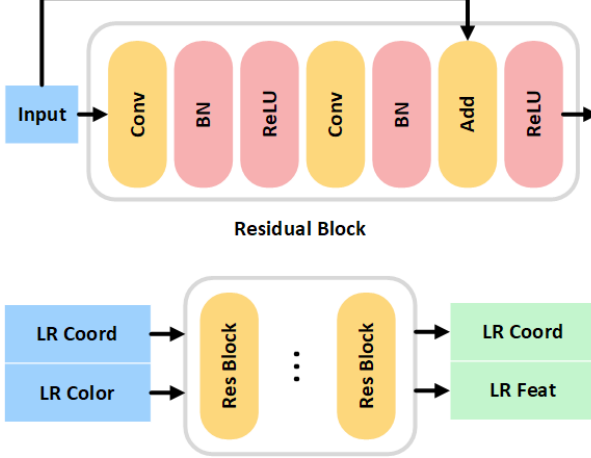


Figure 3. Structure of the feature extraction module.

3.1. Feature Extraction

The feature extraction module extracts LR features from the LR point cloud.

A point in the LR point cloud with index i is defined by a 3D coordinate $p_l^i = (x_i, y_i, z_i)$ and an RGB-format color $c_l^i = (r_i, g_i, b_i)$. The set of LR coordinates $P_l = \{p_l^i\}_i$ can be organized as a tensor with shape $(N_l, 3)$, where N_l is the number of points in LR point cloud. Similarly, the set of LR colors $C_l = \{c_l^i\}_i$ is also a tensor with shape $(N_l, 3)$. Then, LR coordinates and LR colors are combined as one sparse tensor and fed into the feature extraction module. This module outputs a sparse tensor with the same LR coordinates, but deep-learning features attached to these coordinates instead of their original colors. Formally, the point i in the output sparse tensor has the coordinate p_l^i and a deep-learning feature $f_l^i \in \mathbb{R}^K$. Here K is a hyper-parameter about the number of channels. The set of these LR features $F_l = \{f_l^i\}_i$ is represented by a tensor with shape (N_l, K) , and the transformation is as follows.

$$P_l, F_l = \text{FeatureExtraction}(P_l, C_l). \quad (1)$$

We develop a feature extraction module based on sparse convolution. As shown in Fig. 3, the feature extractor has a simple structure with several stacked Residual Blocks [15]. A Residual Block is composed of convolutional layers, batch normalization layers, ReLU activation functions, and a skip connection from the input. These neural network operations are similar with the traditional ones, but supported by a sparse computation backend.

3.2. Feature Expansion

The feature expansion module expands LR features towards the HR point cloud to be HR features.

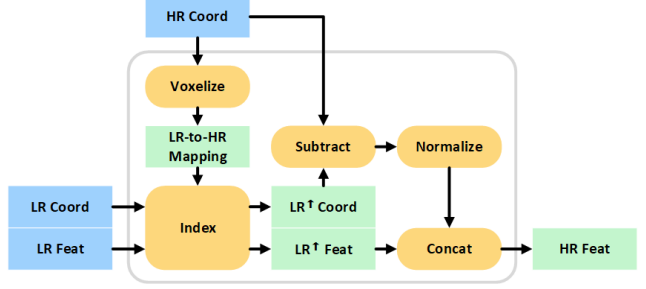


Figure 4. Structure of the feature expansion module. ↑ means that LR data is expanded to have HR shape.

The key of feature expansion is to compute the mapping from LR point cloud to HR point cloud, or the LR-to-HR mapping. Here we make an assumption that LR point cloud is downsampled from HR one via voxelization, which is commonly-used in existing octree-based point cloud compression standards [10]. Voxelization merges several HR points within the same voxel (a small cube) into one LR point at the center of this voxel. From another aspect, one LR point corresponds to several HR points who share the same coordinate after quantization. We can trace the LR-to-HR mapping by recomputing the voxelization, and then expand the LR features using this LR-to-HR mapping.

Define the LR-to-HR mapping function as $m(\cdot)$ and $m(j) = i$ means a HR point with index j is corresponded to a LR point with index i . LR point i has the coordinate p_l^i and deep feature f_l^i , while HR point j has the coordinate p_h^j . Then the HR feature f_h^j is computed as Eq. (2).

$$\begin{aligned} f_h^j &= [f_l^i, \Delta p], \\ \Delta p &= 2 \frac{p_h^j - vp_l^i}{v - 1} - 1, \\ i &= m(j). \end{aligned} \quad (2)$$

Here v is the voxel side length, and $\Delta p \in [-1, 1]$. In other words, the deep feature for a HR point is the concatenation of its corresponding LR point's feature f_l^i and the normalized difference of their coordinates Δp . The explanation to such design is in Sec. 3.3.

An illustration of the feature expansion module is shown in Fig. 4. The module accepts LR coordinates, LR features, and HR coordinates as inputs. It outputs the set of HR features $F_h = \{f_h^j\}_j$ as a tensor with shape (N_h, K) , where N_h is the size of HR point cloud.

3.3. Color Prediction

The color prediction module transforms HR features into the residual details of HR colors.

Denote the residual color predicted by this module with index j as r_h^j . The set of residual HR colors is $R_h = \{r_h^j\}_j$,

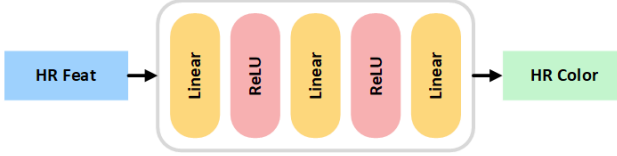


Figure 5. Structure of the color prediction module.

represented by a tensor with shape $(N_h, 3)$. Then the transformation in this step is given as.

$$R_h = \text{ColorPrediction}(F_h). \quad (3)$$

As shown in Fig. 5, the color prediction model is simply a 3-layer Multi Layer Perceptron (MLP). Each layer halves the number of channels, and the last layer reduces it to 3.

The design of our color prediction modules is inspired by recent works about neural implicit function (or neural field) [9, 25]. Neural implicit function is a function parameterized by a neural work, which returns a value given a query position, conditioned on a latent feature. In our case, the LR feature is used as the latent feature to describe local color distribution within a voxel, the normalized coordinate shift is used as query, and the output value is a residual color. Note that we do not adopt the sine-cosine positional encoding used in methods [9, 25] because it brings no improvement.

3.4. Devoxelization

Devoxelization module generates coarse colors as the base of HR colors.

Devoxelization is the inverse operation of voxelization. Specifically, it assigns a LR point's color to all the HR points within the same voxel. When used alone, it incurs blocky artifact as shown in Fig. 6. But in CU-Net, it forces the deep-learning model to spend its capacity on the residual details of colors, which is experimentally proven to benefit the visual quality.

Devoxelization can be efficiently performed by reusing the LR-to-HR mapping computed before. Denote the coarse color generated by devoxelization with index j as d_h^j . Devoxelization is formulated as Eq. (4).

$$d_h^j = c_l^i, \text{ s.t. } i = m(j). \quad (4)$$

Define the final HR color indexed by j as c_h^j . Then as in Eq. (5), the HR color is the summation of a coarse base d_h^j and a deep-learning residual r_h^j .

$$c_h^j = d_h^j + r_h^j. \quad (5)$$

3.5. Complexity Analysis

The feature extraction module is based on sparse convolution. Sparse convolution pre-stores all quantized coordinates using a hash map and only visits occupied positions.

Thus it has an average complexity of $O(N_l)$ in theory. Our feature extractor is implemented using TorchSparse [35] framework, which further improves the empirical efficiency by balancing irregular computation workload and reducing memory footprint.

The feature extraction module contains a voxelization operation, which can be decomposed into one quantization operation over HR coordinates, and one *unique* operation on the quantized coordinates to remove duplicated positions. Since all these operations have linear complexity, the overall complexity of feature expansion is $O(N_h)$.

Color prediction module is a MLP whose complexity is $O(N_h)$. The devoxelization is merely an indexing with $O(N_h)$ complexity.

After all, CU-Net has the complexity of $O(N_l + N_h) = O(N_h)$ for both time and space. Experimental proof of the linear complexity can be found in Sec. 5.2. In comparison, most existing methods have the complexity of $O(N_l^2)$ or even $O(N_h^2)$. Since we always have $N_h \ll N_l^2$, our method is significantly more efficient than existing ones in terms of both runtime and memory.

4. Experiments

4.1. Datasets

We train CU-Net with the FaceScape [37] dataset. FaceScape contains 16,940 human head models captured from 847 subjects performing 20 different expressions. We use 80% of samples for training, 10% for validation, and 10% for evaluation. A FaceScape model is originally a 3D mesh with a 4096×4096 -resolution texture map. We randomly sample 1M points from the surface, and then voxelize them to improve uniformity. The final point cloud lies in a $1000 \times 1000 \times 1000$ space with around 782K points.

We investigate three tasks on the FaceScape dataset - $2 \times$, $5 \times$, and $10 \times$ color upsampling. The original data is down-sampled via voxelization to be the ground truth, and down-sampled again to be the input point cloud. After all, input point clouds for different tasks are the same, but output point clouds are in different scales. The details are given in Tab. 1. Note that the upsampling ratio in our project refers to the space volume, not the number of points as in prior works. Our $10 \times$ upsampling increases the space volume by $10^3 = 1,000 \times$ and the number of points by around $31 \times$.

Table 1. Details of tasks on the FaceScape dataset.

Type	Space	#Points (upsample scale)
Input	100^3	25K
$2 \times$ output	200^3	97K ($\sim 4 \times$)
$5 \times$ output	500^3	445K ($\sim 18 \times$)
$10 \times$ output	1000^3	782K ($\sim 31 \times$)

Beyond FaceScape, we also evaluate color upsampling methods on 6 samples from the MPEG 8i [24] dataset. Each model is a voxelized point cloud residing in a 4096^3 space with around 3.2M points. We study $8\times$ upsampling on this dataset, where the original data is downsampled to be an input point cloud in a 512^3 space with around 236K points.

4.2. Settings

Implementation Details. All programs are implemented using Python. Deep-learning models are based on the PyTorch [27] framework, while sparse convolution is based on TorchSparse [35]. Non-deep-learning methods are implemented by Numpy [14] together with Scikit-learn [28]. All experiments run on Intel Xeon Silver 4214R CPU and NVIDIA RTX 2080ti GPU.

Hyper-Parameters. We optimize CU-Net towards the Mean Square Error (MSE) loss function using an Adam optimizer. The learning rate is 0.001 and decays by 0.1 every 10 epochs. The model is trained for 25 epochs in total with weight decay of 0.0001. The number of residual blocks is 4. For $2\times$ upsampling, we set the number of channels K as 32, and the batch size B as 16. We use $K = 64, B = 8$ for $5\times$ upsampling, and $K = 64, B = 4$ for $10\times$ upsampling.

Metric. We adopt Peak Signal-to-Noise Ratio (PSNR) as the objective metric of visual quality. We evaluate all methods using the average PSNR over RGB channels.

4.3. Baseline Methods

We compare CU-Net with the following baseline methods: devoxelization, Nearest Neighbor (NN), K-Nearest Neighbor (KNN), Weighted Average of Adjacent Neighbors (WAAN) [4]. Devoxelization spreads a LR point’s color towards HR points in the same voxel. NN assigns a point with its nearest neighbor’s color. We omit NN because it’s equivalent to devoxelization in our case. When the point cloud is downsampled via voxelization, a LR point at the center of a voxel is exactly the nearest neighbor of HR points within this voxel. KNN uses the average color of a point’s K ($K=3$ here) nearest neighbors. WAAN collects colors from parent voxels sharing an edge with the target voxel in a weighted average manner. Note that WAAN is originally developed for 2x upsampling in an octree. To apply it for a higher ratio, we generalize it to reject nonadjacent neighbors using ball query, which does not change its behavior for 2x upsampling. We do not compare with FGTV [7] and FSMMR [16], because both methods have prohibitive latency on large-scale points clouds.

5. Result Analysis

5.1. Visual Quality

Quantitative comparisons of color upsampling methods on the FaceScape dataset are shown in Tab. 2. CU-Net

clearly outperforms baseline methods by around 0.8dB for all three tasks. For $2\times$ and $5\times$ upsampling tasks, WAAN performs the best among all baseline methods. For $10\times$ upsampling, KNN is slightly better than other baselines.

We illustrate some results of $10\times$ color upsampling in Fig. 6. Devoxelization or NN generates coarse colors with an acceptable objective score. However, its blocky artifact harms the visual quality. KNN and WAAN can eliminate the artifact and generate smooth colors with higher objective scores. Unfortunately, these interpolation-based methods tend to generate a blurry texture. In contrast, our CU-Net learns to generate sharp and clear details, which improves the visual quality both quantitatively and qualitatively.

5.2. Efficiency

Tab. 2 shows the latency of all methods on both CPU and GPU. Note that all results are measured on one single CPU or GPU, and the GPU latency is the end-to-end latency including both data movement and computation. We can find that devoxelization or NN has the lowest latency on both CPU and GPU. KNN and WAAN run on CPU with a relatively high latency, and it’s nontrivial to apply them on large-scale point clouds on GPU. CU-Net is able to run on CPU but will gain a significant speedup on GPU. When deployed on GPU, CU-Net achieves real-time (>30 FPS) inference by having about 77 FPS for $2\times$ upsampling and 45 FPS for $5\times$ upsampling. CU-Net can even achieve 34 FPS for $10\times$ upsampling, which requires the model to predict around 782K colors for each object.

GPU latency of CU-Net has a strong (the coefficient of determination $R^2 = 0.9948$) linearity with the number of HR points in Tab. 1. It agrees with CU-Net’s $O(N_h)$ complexity in theory. The CPU latency has a sub-linear relationship with the number of HR points, as the implementation of deep learning operations on CPU is different from GPU.

CU-Net is memory-efficient to process around 3.2M points within a single GPU card, when it’s applied to the MPEG 8i samples in Sec. 5.4. According to Tab. 2, CU-Net has a small model size from 0.77 to 3.01 MB, which is acceptable for most storage devices.

In summary, CU-Net has satisfying efficiency in terms of runtime, memory consumption, and storage space.

5.3. Arbitrary-Ratio Upsampling

As discussed in Sec. 3.3, CU-Net’s color prediction module is a neural implicit function that receives a position and predicts a color. Since CU-Net can accept any number of query positions, it supports an arbitrary upsampling ratio.

To verify this property, we train CU-Net towards one upsampling ratio (train ratio) and evaluates it on another ratio (test ratio). According to Tab. 3, CU-Net trained for $5\times$ upsampling can be used for a lower ratio like $2\times$, or a higher

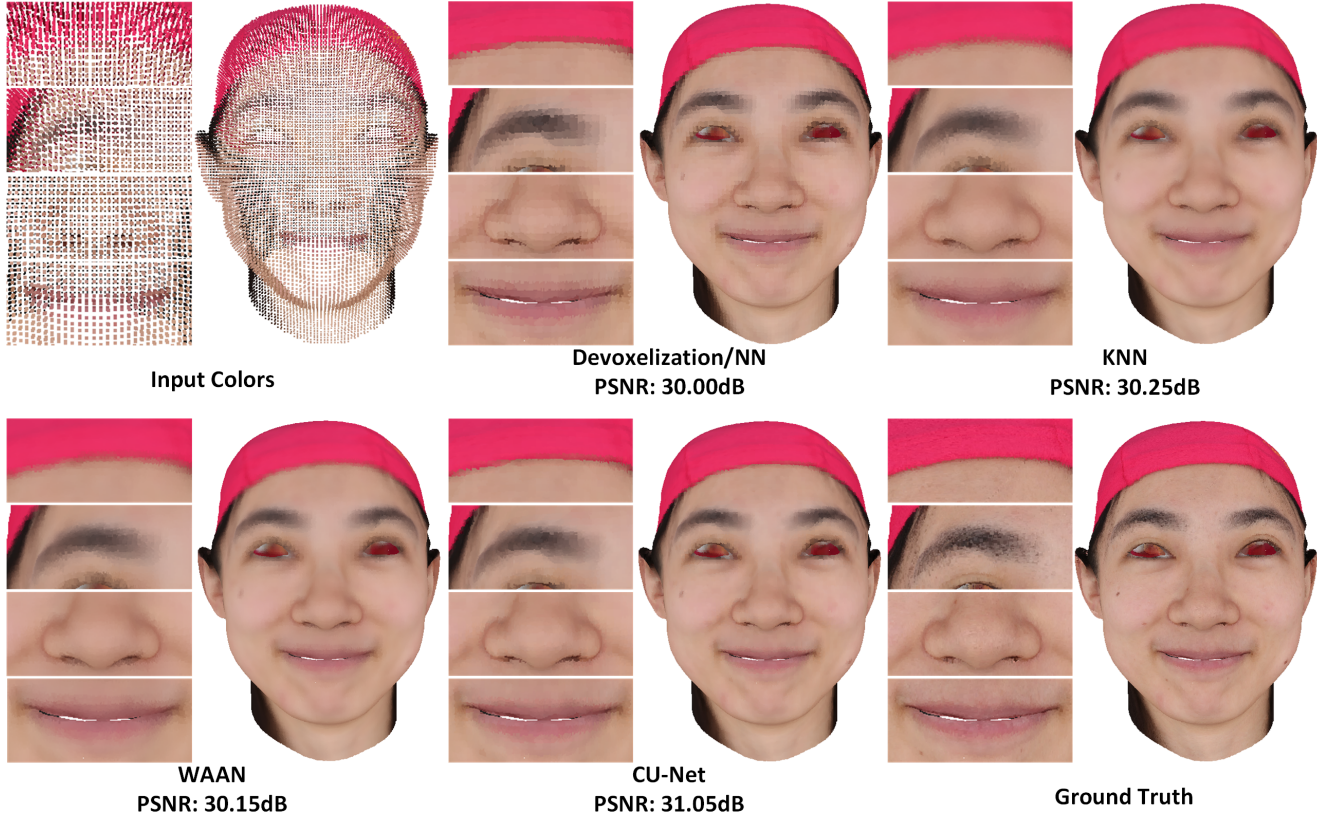


Figure 6. Results of $10\times$ color upsampling on the 122_smile model from the FaceScape dataset. **Best viewed zoomed in.**

Table 2. Color upsampling results on the FaceScape dataset.

Ratio	Method	PSNR (dB)	Model Size (MB)	CPU Latency (ms)	GPU Latency (ms)
2 \times	Devox/NN	31.23	-	13.87	1.73
	KNN	30.62	-	224.37	-
	WAAN [4]	31.33	-	323.40	-
	CU-Net (ours)	32.09	0.77	360.57	13.02
5 \times	Devox/NN	30.42	-	38.14	4.69
	KNN	30.49	-	960.52	-
	WAAN [4]	30.65	-	1388.81	-
	CU-Net (ours)	31.32	3.01	722.74	22.17
10 \times	Devox/NN	30.37	-	60.07	7.39
	KNN	30.52	-	1665.31	-
	WAAN [4]	30.43	-	2383.21	-
	CU-Net (ours)	31.26	3.01	875.04	29.06

ratio like $10\times$. Actually, CU-Net trained for $5\times$ achieves the best performance in $2\times$. The model trained for $10\times$ can also adapt to any ratio. However, as shown in Fig. 7, this model introduces stripes when generalized to other ratios. This is probably because CU-Net is trivialized during the training process of $2\times$ upsampling, where it only learns

to expand a feature towards $2^3 = 8$ positions. In contrast, CU-Net trained for higher ratios needs to spread a feature towards $5^3 = 125$ or $10^3 = 1000$ positions. This forces the model to learn an approximately continuous color field where the model can sample from any position.

In a nutshell, CU-Net trained for a high upsampling ratio



Figure 7. Arbitrary-ratio upsampling results of CU-Net on the 212_anger model from the FaceScape dataset.

Table 3. Arbitrary-ratio upsampling results of CU-Net on the FaceScape dataset, measured in PSNR (dB).

Train \ Test Ratio	2×	5×	10×
2×	32.09	30.65	30.61
5×	32.12	31.32	31.25
10×	32.10	31.32	31.26

can be used for an arbitrary ratio without performance loss.

Table 4. Results of 8× color upsampling on the MPEG 8i dataset, measured in PSNR (dB).

Model	Devox /NN	KNN	WAAN [4]	CU-Net (ours)
Boxer	38.95	39.47	39.57	41.30
LongDress	29.53	29.62	29.63	31.06
Loot	39.04	39.69	39.79	42.56
RedBlack	34.30	34.96	35.04	35.90
Soldier	34.77	35.29	35.34	37.86
ThaiDancer	27.20	26.85	26.78	27.91

5.4. Generalization

To verify the generalization ability and robustness of CU-Net, a model trained for 10× upsampling on the FaceScape dataset is applied to 8× upsampling on the MPEG 8i dataset. According to the quantitative results in Tab. 4, CU-Net dramatically outperforms other methods for all 6 samples. As illustrated in Fig. 8, devoxelization or NN incurs blocky artifact. KNN and WAAN output overly smooth textures. While CU-Net manages to generate complicated colors on the face and clothes. This proves that CU-Net can generalize to unseen objects with an arbitrary

upsampling ratio.

6. Conclusion

Point cloud color upsampling is demanded but long ignored in AR/VR and telepresence scenarios. In this paper we present CU-Net, the first deep-learning color up-sampling model. CU-Net adopts a feature extraction module based on sparse convolution, an efficient feature expansion module, a color prediction module analogous to neural implicit function, and a devoxelization module for coarse colors. CU-Net achieves $O(N_h)$ time and space complexity, which is theoretically better than most existing methods with quadratic complexity. Through abundant experiments, we show that CU-Net outperforms baseline methods in visual quality while having satisfying runtime, memory, and storage efficiency. Besides, CU-Net supports arbitrary-ratio upsampling and is robust to unseen dataset.

References

- [1] Anique Akhtar, Zhu Li, Geert Van der Auwera, Li Li, and Jianle Chen. Pu-dense: Sparse tensor-based point cloud geometry upsampling. *IEEE Transactions on Image Processing*, 31:4133–4148, 2022. [1](#), [2](#), [3](#)
- [2] M. Alexa, J. Behr, D. Cohen-Or, S. Fleishman, D. Levin, and C.T. Silva. Computing and rendering point set surfaces. *IEEE Transactions on Visualization and Computer Graphics*, 9(1):3–15, 2003. [2](#)
- [3] Evangelos Alexiou, Evgeniy Upenik, and Touradj Ebrahimi. Towards subjective quality assessment of point cloud imaging in augmented reality. In *2017 IEEE 19th International Workshop on Multimedia Signal Processing (MMSP)*, pages 1–6, 2017. [1](#)
- [4] Tomás M. Borges, Diogo C. Garcia, and Ricardo L. de Queiroz. Fractional super-resolution of voxelized point clouds. *IEEE Transactions on Image Processing*, 31:1380–1390, 2022. [2](#), [3](#), [6](#), [7](#), [8](#)

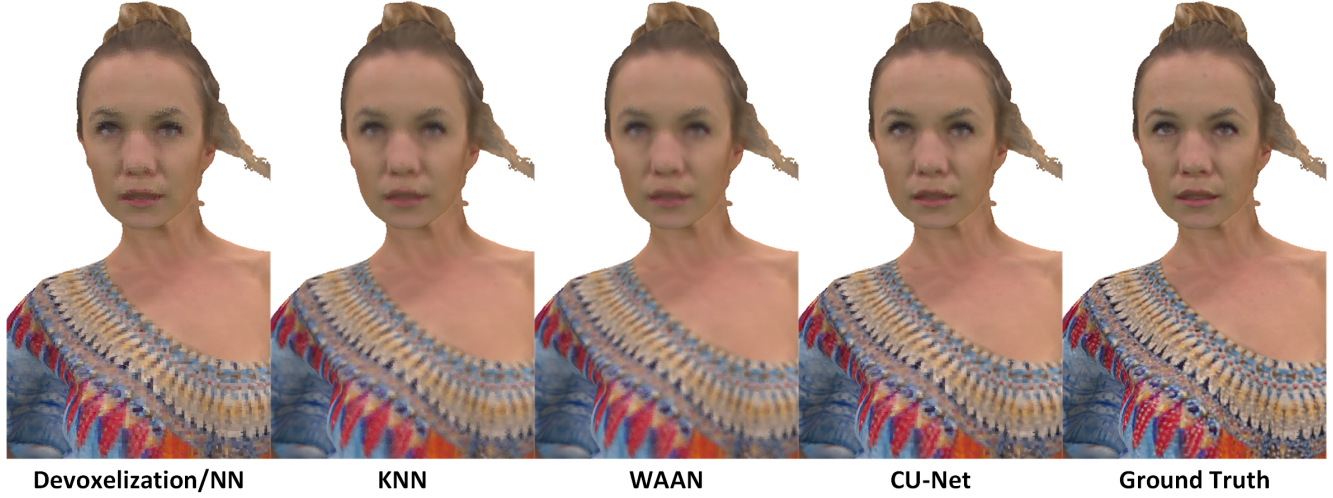


Figure 8. Results of $8 \times$ color upsampling on the LongDress model from the MPEG 8i dataset.

- [5] Xu Cao and Katashi Nagao. Point cloud colorization based on densely annotated 3d shape dataset. In Ioannis Kompatiridis, Benoit Huet, Vasileios Mezaris, Cathal Gurrin, Wen-Huang Cheng, and Stefanos Vrochidis, editors, *MultiMedia Modeling*, pages 436–446, Cham, 2019. Springer International Publishing. [3](#)
- [6] Christopher Choy, JunYoung Gwak, and Silvio Savarese. 4d spatio-temporal convnets: Minkowski convolutional neural networks. In *Proceedings of the IEEE/CVF Conference on Computer Vision and Pattern Recognition (CVPR)*, June 2019. [2](#)
- [7] Chinthaka Dinesh, Gene Cheung, and Ivan V Bajić. Super-resolution of 3d color point clouds via fast graph total variation. In *ICASSP 2020 - 2020 IEEE International Conference on Acoustics, Speech and Signal Processing (ICASSP)*, pages 1983–1987, 2020. [2, 3, 6](#)
- [8] John V Draper, David B Kaber, and John M Usher. Telepresence. *Human factors*, 40(3):354–375, 1998. [1](#)
- [9] Wanquan Feng, Jin Li, Hongrui Cai, Xiaonan Luo, and Juyong Zhang. Neural points: Point cloud representation with neural fields for arbitrary upsampling. In *Proceedings of the IEEE/CVF Conference on Computer Vision and Pattern Recognition (CVPR)*, pages 18633–18642, June 2022. [1, 2, 3, 5](#)
- [10] D. Graziosi, O. Nakagami, S. Kuma, A. Zaghetto, T. Suzuki, and A. Tabatabai. An overview of ongoing point cloud compression standardization activities: video-based (v-pcc) and geometry-based (g-pcc). *APSIPA Transactions on Signal and Information Processing*, 9:e13, 2020. [1, 4](#)
- [11] Kaiwen Guo, Peter Lincoln, Philip Davidson, Jay Busch, Xueming Yu, Matt Whalen, Geoff Harvey, Sergio Orts-Escalano, Rohit Pandey, Jason Dourgarian, Danhang Tang, Anastasia Tkach, Adarsh Kowdle, Emily Cooper, Mingsong Dou, Sean Fanello, Graham Fyffe, Christoph Rhemann, Jonathan Taylor, Paul Debevec, and Shahram Izadi. The relightables: Volumetric performance capture of humans with realistic relighting. 38(6), nov 2019. [1](#)
- [12] Meng-Hao Guo, Jun-Xiong Cai, Zheng-Ning Liu, Tai-Jiang Mu, Ralph R Martin, and Shi-Min Hu. Pct: Point cloud transformer. *Computational Visual Media*, 7(2):187–199, 2021. [2](#)
- [13] Bing Han, Xinyun Zhang, and Shuang Ren. Pu-gacnet: Graph attention convolution network for point cloud upsampling. *Image and Vision Computing*, 118:104371, 2022. [1, 2, 3](#)
- [14] Charles R. Harris, K. Jarrod Millman, Stéfan J. van der Walt, Ralf Gommers, Pauli Virtanen, David Cournapeau, Eric Wieser, Julian Taylor, Sebastian Berg, Nathaniel J. Smith, Robert Kern, Matti Picus, Stephan Hoyer, Marten H. van Kerkwijk, Matthew Brett, Allan Haldane, Jaime Fernández del Río, Mark Wiebe, Pearu Peterson, Pierre Gérard-Marchant, Kevin Sheppard, Tyler Reddy, Warren Weckesser, Hameer Abbasi, Christoph Gohlke, and Travis E. Oliphant. Array programming with NumPy. *Nature*, 585(7825):357–362, Sept. 2020. [6](#)
- [15] Kaiming He, Xiangyu Zhang, Shaoqing Ren, and Jian Sun. Deep residual learning for image recognition. In *Proceedings of the IEEE Conference on Computer Vision and Pattern Recognition (CVPR)*, June 2016. [4](#)
- [16] Viktoria Heimann, Andreas Spruck, and André Kaup. Frequency-selective mesh-to-mesh resampling for color upsampling of point clouds. In *2021 IEEE 23rd International Workshop on Multimedia Signal Processing (MMSP)*, pages 1–6, 2021. [2, 3, 6](#)
- [17] Hui Huang, Dan Li, Hao Zhang, Uri Ascher, and Daniel Cohen-Or. Consolidation of unorganized point clouds for surface reconstruction. *ACM Trans. Graph.*, 28(5):1–7, dec 2009. [2](#)
- [18] Hui Huang, Shihao Wu, Minglun Gong, Daniel Cohen-Or, Uri Ascher, and Hao (Richard) Zhang. Edge-aware point set resampling. *ACM Trans. Graph.*, 32(1), feb 2013. [2](#)
- [19] Yuki Ishida, Yoshitsugu Manabe, and Noriko Yata. Colored point cloud completion for a head using adversarial rendered image loss. *Journal of Imaging*, 8(5), 2022. [3](#)

[20] Ruihui Li, Xianzhi Li, Chi-Wing Fu, Daniel Cohen-Or, and Pheng-Ann Heng. Pu-gan: A point cloud upsampling adversarial network. In *Proceedings of the IEEE/CVF International Conference on Computer Vision (ICCV)*, October 2019. 1, 3

[21] Ruihui Li, Xianzhi Li, Pheng-Ann Heng, and Chi-Wing Fu. Point cloud upsampling via disentangled refinement. In *Proceedings of the IEEE/CVF Conference on Computer Vision and Pattern Recognition (CVPR)*, pages 344–353, June 2021. 1, 3

[22] Yaron Lipman, Daniel Cohen-Or, David Levin, and Hillel Tal-Ezer. Parameterization-free projection for geometry reconstruction. *ACM Trans. Graph.*, 26(3):22–es, jul 2007. 2

[23] Jitao Liu, Songmin Dai, and Xiaoqiang Li. Pccn:point cloud colorization network. In *2019 IEEE International Conference on Image Processing (ICIP)*, pages 3716–3720, 2019. 3

[24] Maja Krivokuća, Philip A. Chou, and Patrick Savill. 8i voxelized surface light field (8ivslf) dataset. *ISO/IEC JTC1/SC29 WG11 (MPEG) input document m42914*, July 2018. 6

[25] Ben Mildenhall, Pratul P. Srinivasan, Matthew Tancik, Jonathan T. Barron, Ravi Ramamoorthi, and Ren Ng. Nerf: Representing scenes as neural radiance fields for view synthesis. In Andrea Vedaldi, Horst Bischof, Thomas Brox, and Jan-Michael Frahm, editors, *Computer Vision – ECCV 2020*, pages 405–421, Cham, 2020. Springer International Publishing. 2, 3, 5

[26] Sergio Orts-Escalano, Christoph Rhemann, Sean Fanello, Wayne Chang, Adarsh Kowdle, Yury Degtyarev, David Kim, Philip L. Davidson, Sameh Khamis, Mingsong Dou, Vladimir Tankovich, Charles Loop, Qin Cai, Philip A. Chou, Sarah Mennicken, Julien Valentin, Vivek Pradeep, Shenlong Wang, Sing Bing Kang, Pushmeet Kohli, Yuliya Lutchny, Cem Keskin, and Shahram Izadi. Holoportation: Virtual 3d teleportation in real-time. In *Proceedings of the 29th Annual Symposium on User Interface Software and Technology, UIST ’16*, page 741–754, New York, NY, USA, 2016. Association for Computing Machinery. 1

[27] Adam Paszke, Sam Gross, Francisco Massa, Adam Lerer, James Bradbury, Gregory Chanan, Trevor Killeen, Zeming Lin, Natalia Gimelshein, Luca Antiga, Alban Desmaison, Andreas Kopf, Edward Yang, Zachary DeVito, Martin Raison, Alykhan Tejani, Sasank Chilamkurthy, Benoit Steiner, Lu Fang, Junjie Bai, and Soumith Chintala. Pytorch: An imperative style, high-performance deep learning library. In H. Wallach, H. Larochelle, A. Beygelzimer, F. d’Alché-Buc, E. Fox, and R. Garnett, editors, *Advances in Neural Information Processing Systems 32*, pages 8024–8035. Curran Associates, Inc., 2019. 6

[28] F. Pedregosa, G. Varoquaux, A. Gramfort, V. Michel, B. Thirion, O. Grisel, M. Blondel, P. Prettenhofer, R. Weiss, V. Dubourg, J. Vanderplas, A. Passos, D. Cournapeau, M. Brucher, M. Perrot, and E. Duchesnay. Scikit-learn: Machine learning in Python. *Journal of Machine Learning Research*, 12:2825–2830, 2011. 6

[29] Charles R. Qi, Hao Su, Kaichun Mo, and Leonidas J. Guibas. Pointnet: Deep learning on point sets for 3d classification and segmentation. In *Proceedings of the IEEE Conference on Computer Vision and Pattern Recognition (CVPR)*, July 2017. 2

[30] Charles Ruizhongtai Qi, Li Yi, Hao Su, and Leonidas J Guibas. Pointnet++: Deep hierarchical feature learning on point sets in a metric space. In I. Guyon, U. Von Luxburg, S. Bengio, H. Wallach, R. Fergus, S. Vishwanathan, and R. Garnett, editors, *Advances in Neural Information Processing Systems*, volume 30. Curran Associates, Inc., 2017. 2, 3

[31] Guocheng Qian, Abdulellah Abualshour, Guohao Li, Ali Thabet, and Bernard Ghanem. Pu-gcn: Point cloud upsampling using graph convolutional networks. In *Proceedings of the IEEE/CVF Conference on Computer Vision and Pattern Recognition (CVPR)*, pages 11683–11692, June 2021. 1, 2, 3

[32] Yue Qian, Junhui Hou, Sam Kwong, and Ying He. Deep magnification-flexible upsampling over 3d point clouds. *IEEE Transactions on Image Processing*, 30:8354–8367, 2021. 1, 3

[33] Shi Qiu, Saeed Anwar, and Nick Barnes. Pu-transformer: Point cloud upsampling transformer, 2021. 1, 3

[34] Takayuki Shinohara, Haoyi Xiu, and Masashi Matsuoka. Point2color: 3d point cloud colorization using a conditional generative network and differentiable rendering for airborne lidar. In *Proceedings of the IEEE/CVF Conference on Computer Vision and Pattern Recognition (CVPR) Workshops*, pages 1062–1071, June 2021. 3

[35] Haotian Tang, Zhijian Liu, Xiuyu Li, Yujun Lin, and Song Han. Torchsparse: Efficient point cloud inference engine. In D. Marculescu, Y. Chi, and C. Wu, editors, *Proceedings of Machine Learning and Systems*, volume 4, pages 302–315, 2022. 2, 5, 6

[36] Yue Wang, Yongbin Sun, Ziwei Liu, Sanjay E. Sarma, Michael M. Bronstein, and Justin M. Solomon. Dynamic graph cnn for learning on point clouds. *ACM Trans. Graph.*, 38(5), oct 2019. 2, 3

[37] Haotian Yang, Hao Zhu, Yanru Wang, Mingkai Huang, Qiu Shen, Ruigang Yang, and Xun Cao. Facescape: A large-scale high quality 3d face dataset and detailed riggable 3d face prediction. In *Proceedings of the IEEE/CVF Conference on Computer Vision and Pattern Recognition (CVPR)*, June 2020. 5

[38] Shuquan Ye, Dongdong Chen, Songfang Han, Ziyu Wan, and Jing Liao. Meta-pu: An arbitrary-scale upsampling network for point cloud. *IEEE Transactions on Visualization and Computer Graphics*, pages 1–1, 2021. 1, 3

[39] Wang Yifan, Shihao Wu, Hui Huang, Daniel Cohen-Or, and Olga Sorkine-Hornung. Patch-based progressive 3d point set upsampling. In *Proceedings of the IEEE/CVF Conference on Computer Vision and Pattern Recognition (CVPR)*, June 2019. 1, 3

[40] Kevin Yu, Gleb Gorbachev, Ulrich Eck, Frieder Pankratz, Nassir Navab, and Daniel Roth. Avatars for teleconsultation: Effects of avatar embodiment techniques on user perception in 3d asymmetric telepresence. *IEEE Transactions on Visualization and Computer Graphics*, 27(11):4129–4139, 2021. 1

- [41] Lequan Yu, Xianzhi Li, Chi-Wing Fu, Daniel Cohen-Or, and Peng-Ann Heng. Pu-net: Point cloud upsampling network. In *Proceedings of the IEEE Conference on Computer Vision and Pattern Recognition (CVPR)*, June 2018. [1](#), [3](#)
- [42] Anlan Zhang, Chendong Wang, Bo Han, and Feng Qian. YuZu: Neural-Enhanced volumetric video streaming. In *19th USENIX Symposium on Networked Systems Design and Implementation (NSDI 22)*, pages 137–154, Renton, WA, Apr. 2022. USENIX Association. [1](#), [2](#), [3](#)
- [43] Yizhong Zhang, Jiaolong Yang, Zhen Liu, Ruicheng Wang, Guojun Chen, Xin Tong, and Baining Guo. Virtualcube: An immersive 3d video communication system. *IEEE Transactions on Visualization and Computer Graphics*, 28(5):2146–2156, 2022. [1](#)
- [44] Hengshuang Zhao, Li Jiang, Jiaya Jia, Philip H.S. Torr, and Vladlen Koltun. Point transformer. In *Proceedings of the IEEE/CVF International Conference on Computer Vision (ICCV)*, pages 16259–16268, October 2021. [2](#)